A combined dynamical and statistical downscaling technique to reduce biases in climate projections: An example for winter precipitation and snowpack in the western United States

R. Li[1, 2], S.-Y. Wang[1, 2], R. R. Gillies[1, 2]

(1) Utah Climate Center, Utah State University, Logan, UT, USA
(2) Department of Plants, Soils, and Climate, Utah State University, Logan, UT, USA

Emails: lirong18@gmail.com, simon.wang@usu.edu, Robert.Gillies@usu.edu

Abstract

Large biases associated with climate projections are problematic when it comes to their regional application in the assessment of water resources and ecosystems. Here, we demonstrate a method that can reduce systematic biases in regional climate projections. The global and regional climate models employed to demonstrate this technique are the Community Climate System Model (CCSM) and the Weather Research and Forecasting (WRF) model, respectively. The method first utilized a statistical regression technique and a global reanalysis dataset to correct biases in the CCSM-simulated variables (e.g., temperature, geopotential height, specific humidity, and winds) that are subsequently used to drive the WRF model. The WRF simulations were conducted for the western United States and were driven with a) global reanalysis, b) original CCSM, and c) bias-corrected CCSM data. The bias-corrected CCSM data led to a more realistic regional climate simulation of precipitation and associated atmospheric dynamics, as well as snow water equivalent (SWE) in comparison to the original CCSM-driven WRF simulation. Since most climate applications rely on existing global model output as the forcing data (i.e. they cannot re-run or change the global model), which often contain large biases, this effective and economical method provides a useful tool to reduce biases in regional

climate downscaling simulations of water resource variables.

Keywords: Regional climate modeling, dynamical downscaling, snowpack, precipitation, western U.S., climate change, snow water equivalent

1. Introduction

The assessment of, and adaptation to, future water resources depends heavily upon reliable climate simulations of precipitation, snowpack, and temperature. Deriving regional climate information from coupled atmosphere–ocean general circulation model (CGCMs) projections by using regional climate models (RCMs), namely dynamical downscaling, has become a common practice (Hayhoe et al. 2004; Wood et al. 2004; Wilby et al. 1998; Gutierrez et al. 2013; Hewitson and Crane 1996). Dynamical downscaling generates physics-based representations of future climate processes that also account for the changing dynamics in the climate system; this is its advantage over statistical downscaling (Leung et al. 2003a; Leung et al. 2003b; Liang et al. 2008). However, certain climate variables, especially snowpack and precipitation, are particularly difficult to simulate accurately (Salzmann and Mearns 2012; Rasmussen et al. 2011; Mearns et al. 2013; Mearns et al. 2012; Pielke 2013), and it is impossible to correct their large biases through either dynamical or statistical methods alone.

Generally, biases in dynamical downscaling originate from two sources: (1) inadequate representation of the physical processes in the RCMs, and (2) biases propagated into the RCMs from the "parent" CGCMs (Pielke and Wilby, 2012). Since RCMs and dynamical downscaling are expensive in terms of model development and computing time, some studies that require regional climate information tend to utilize existing simulations provided by a handful of modeling centers, e.g., those participating in the North American Regional Climate Change Assessment Program (NARCCAP; Mearns et al. 2012). Consequently, these studies are forced to work with both types of biases in the existing climate simulations. Since CGCM simulations are also complex and computationally expensive, most studies that perform their own regional climate simulations have to rely upon national centers and coordinated projects (e.g., the Coupled Model Intercomparison Project Phase 5 (CMIP5)) (Taylor et al. 2012) for CGCM data to provide boundary conditions to RCMs. However, such CGCM-derived boundary conditions contain model-specific and often large biases; these also degrade the downscaled simulation results (e.g., Wang et al. 2009).

Given the aforementioned problems that exist in both regional and global climate models, we sought to develop an effective and economical procedure to improve regional climate downscaling. For this paper, we focused on downscaled precipitation and snowpack projections in the semi-arid western United States, where reliable assessment of future changes in water resources has been a challenge. For example, existing simulations in the western U.S. such as NARCCAP (50 km resolution) tended to predict too much winter precipitation (Mearns et al. 2012; Wang et al. 2009), too little SWE (Salzmann and Mearns 2012), and inconsistent long-term trends by different models (Salzmann and Mearns 2012). In addition, the simulation of snow water equivalent (SWE) generally requires the use of high (< 10 km) resolution model runs (Rasmussen et al. 2011; Jin and Wen 2012); this is often prohibitively expensive. Here, we present results from a combined statistical and dynamical technique, first introduced by Jin et al. (2011), that can reduce biases resulting from both inadequate RCM physics and biased CGCM boundary conditions without the expense of having to use fine resolutions.

The paper introduces the bias-correction method applied to the CGCM data that are subsequently used as boundary conditions by a RCM in Section 2, followed by the RCM simulation results of precipitation, SWE and temperature in Section 3. A summary with conclusions is given in Section 4.

2. Methods

For the lateral boundary conditions we utilized the CCSM3 (the Community Climate System Model) simulations forced with the IPCC A2 emissions (the higher end but not the highest), which were described in the fourth assessment report (Nakicenvoic et al. 2000). The CCSM3 output was obtained from the 3rd phase of CMIP. Although the newer version model (CCSM4) had been released in 2013, we used the older version (CCSM3) in order to demonstrate the effectiveness of the bias correction technique since this precludes the use of any particular global model iterations. Hereafter the global model output is referred to as CCSM.

Biases in the CCSM data can propagate into the WRF simulation and degrade the downscaled climate projections, and thus need to be corrected before feeding into the WRF model. The approach used in this study to correct biases in the CCSM data is based upon Dettinger et al. (2004) and Miller et al. (2008). The key point here is to maintain physical consistency among essential variables used to drive WRF, including temperature (T), specific humidity (Q), surface pressure (P), geopotential height (Z), and winds (U and V). Following Jin et al. (2011), the 6-hourly CCSM's temperature, specific humidity, and surface pressure, which are relatively independent, were corrected using regression coefficients of biases in each variable for each model point at each pressure level. These regression coefficients of biases were calculated using linear regression with the observation-based NCEP Reanalysis (Kalnay et al. 1996) over the years 1948-1999. Then the bias-corrected T, Q, and P were used to compute the geopotential height (Z) based on hydrostatic and other physical relationships among these variables (Holton 1992). The "reconstructed" Z was subsequently used to calculate the geostrophic wind ($\vec{V}_g$). Next, in order to compute the ageostrophic wind ($\vec{V}_a$), which is more difficult to calculate since the percentage of ageostrophic wind in total wind is large near the surface, the NCEP Reanalysis winds were first decomposed into the geostrophic and ageostrophic components. Then a regression model was developed between the NCEP ageostrophic wind and corrected T and Q (i.e. the main drivers of the ageostrophic effect). The regression model was subsequently applied to generate $\vec{V}_a$, which was then combined with $\vec{V}_g$ to produce the bias-corrected total wind $\vec{V}$. Such a bias-corrected total wind field was then applied onto the boundary conditions driving the RCM simulations.

We used the Weather Research and Forecasting model (WRF) version 3.2.1 (http://www.wrf-model.org/index.php) coupled with the Community Land Model (CLM) version 3.5 (Jin and Wen 2012; Subin et al. 2011) as the RCM. The coupling of the CLM has been shown to improve WRF's simulation of snow, soil, and vegetation processes (Jin and Wen 2012; Subin et al. 2011). Since WRF has an array of physics scheme options and each scheme tends to introduce particular biases, sensitivity tests were undertaken to obtain an optimal combination of physics schemes that were effective in simulating the most realistic precipitation and air temperatures over the western U.S. The sensitivity tests were performed using the NCEP Reanalysis (as the boundary conditions), and the identified optimal set of physics schemes is listed in Table 1. The simulations were performed at a spatial resolution of 50 km over the domain (ref., Figure 1).

A set of historical (1969-1999) WRF simulations were then undertaken with lateral boundary conditions being supplied by a) the NCEP Reanalysis, b) the original CCSM (not bias-corrected), and c) the bias-corrected CCSM data. Two additional simulations were conducted for the 2001-2010 period using the original and bias-corrected CCSM data. Lastly, WRF simulations were carried out for the mid-21st Century (2056-2065) using both the original and bias-corrected CCSM data. The simulations for the 2001-2010 and 2056-2065 periods were driven with the transient simulation of CCSM (i.e., in forecasting mode). We focused on the winter snow season (i.e. January-March) in the western U.S. Each of the simulations included a model spin-up over four months from September 1 to December 31 of the previous year.

3. Results

The observed mean precipitation for January-March (JFM) during 1969-1999, derived from the Parameter-elevation Regressions on Independent Slopes Model (PRISM) data (Daly et al. 1994), is shown in Figure 1a. Visually, the NCEP-driven simulation of precipitation (Figure 1b) is in good agreement with the observation. Quantitatively, the root mean square deviation (RMSD) of the JFM precipitation was 43 mm/month over the western U.S. domain (with respect to PRISM). The NCEP-driven simulation serves as the upper bound for model performance (Mearns et al. 2013; Mearns et al. 2012; Pielke 2013). In comparison, the original CCSM-driven simulation resulted in significant wet biases throughout the western U.S. (Figure 1c), increasing the RMSD to

80 mm/month. Since both the NCEP-driven and the original CCSM-driven simulations used exactly the same physics schemes in WRF, the differences in simulated precipitation could only be caused by the disparities in WRF input data between the two simulations. This means that the original CCSM data have significant biases that were passed through the WRF model. The bias-corrected CCSM-driven simulation (Figure 1d) reduced the wet bias and lessened the RMSD to 70 mm/month, mostly in the southwestern U.S. This means that although there are still biases in WRF-simulated precipitation resulting from imperfect representations of physics in the WRF model and biases in its forcing data, the bias-correction method did improve the WRF simulation.

The more important questions posed are: (a) how may the JFM precipitation change in response to such a bias correction? (b) how does it affect the mountain snowpack projection? To examine these questions, we plotted the JFM precipitation differences between future (2056-2065) and current (2001-2010) periods; these are shown in Figures 1e and 1f. The results reveal a marked difference between the original and bias-corrected CCSM-driven simulations and this is emphasized by a spatial correlation coefficient (R) of only 0.07. In the original CCSM-driven simulation, the change in the JFM precipitation exhibits a widespread increase across much of the western U.S. with most of the increase covering a 35°-46°N latitudinal band. Northward of 46°N decreased precipitation was simulated. In the bias-corrected CCSM-driven simulation, however, the precipitation change reveals a north-south dipole with a large increase in the northwestern states and a slight decrease in the southwestern states.

It was found that the precipitation differences corresponded closely to the circulation changes. Figures 2a-c show the mean JFM wind fields at 200 hPa for the

1969-1999 period derived from the (a) NCEP-driven, (b) original CCSM-driven, and (c) bias-corrected CCSM-driven simulations. Compared to the NCEP-driven simulation (Figure 2a), the original CCSM-driven simulation produced considerably stronger winds over most of the domain and induced a pseudo jet streak near 50°N (Figure 2b). In contrast, wind fields in the bias-corrected CCSM-driven simulation (Figure 2c) were in better agreement with the NCEP-driven simulation, though the wind speed remained slightly higher over the interior West. Overly strong westerly winds in both the original and bias-corrected CCSM-driven simulations were observed throughout the troposphere (not shown) and this likely caused the overly wet biases along the windward side of the mountains, as is revealed in Figure 1 and found occurred in NARCCAP model simulations by Wang et al. (2009).

The wind changes at 200 hPa between the 2056-2065 and 2001-2010 periods also showed a marked difference between the original CCSM-driven (Figure 2d) and bias-corrected CCSM-driven (Figure 2e) simulations. Both simulations produced an anomalous trough over the western U.S. sandwiched between two anomalous ridges to the west and east. In the bias-corrected CCSM-driven simulation, the trough was displaced further north, but the wind speed was much reduced when compared to the original CCSM-driven simulation. At 600 hPa, the differences in the wind anomalies (Figures 2f and 2g) are similar to those at 200 hPa, suggesting a barotropic structure (i.e. vertically uniform). In the bias-corrected CCSM-driven simulation, the cyclonic center was positioned at the U.S.-Canadian border and the westerly wind anomalies were moved northwestward; this led to the northward displacement of the precipitation anomalies (Figure 1f). Apparently, the bias-corrected boundary conditions produced a marked impact on the "downscaled" circulation simulations, which, in turn, could and did alter the precipitation projections.

Any changes in projected winter precipitation would directly affect projections of mountain snowpack – a crucial water resource in the region as was noted earlier. To investigate further, we focused on four major mountain regions: (1) the Cascade Range, (2) the Bitterroot Range, (3) the Wasatch Range, and (4) the Colorado Rockies; these are delineated by boxes labeled 1, 2, 3, and 4 in Figure 1b. For evaluation purposes we utilized the Snowpack Telemetry Network (SNOTEL) observations; there are respectively 46, 32, 79, and 71 SNOTEL stations within the four mountain regions. Figures 3a-d show the time series of the April 1 snow water equivalent (SWE) derived from the SNOTEL, NCEP-driven, original CCSM-driven, and bias-corrected CCSM-driven simulations, overlaid with the linear trends. Over each mountainous region, the mean values of the 2001-2010 and 2056-2065 periods in each simulation are connected by a dashed line to indicate future changes.

Figures 3a-d show that the original CCSM-driven simulation yielded marked increasing SWE trends in all four regions; this is not in agreement with the observed decreases of SWE in Regions 2, 3 and 4. The decreasing SWE in Regions 2, 3 and 4 has been noticed in previous studies (Christensen et al. 2004; Gillies et al. 2012; Howat and Tulaczyk 2005). By contrast, in all four regions, the bias-corrected CCSM-driven simulations produced SWE trends that are in better agreement with the SNOTEL observations. The trend lines in the NCEP-driven simulations were also aligned more closely with the SNOTEL observations. Regarding future projections, i.e. from 2001-2010 to 2056-2065, the bias-corrected CCSM-driven simulations indicate a future decline in SWE in each region; this is in contrast to the original CCSM-driven simulation, which did not produce any significant SWE change in all regions with the exception of the Cascades (Region 1). It is also noted that the SWEs tend to be lower in the WRF simulations in comparison to the observations. Such underestimations in SWE are expected because most SNOTEL stations are sited at high-elevation in the mountains where snow tends to accumulate, whereas the averaging of the modeled SWEs over a box domain includes low elevation locations (e.g., valley) where there are less snow amounts.

To explain the differences in the SWE trends, Figure 4 shows the trends of the JFM precipitation for the four mountainous regions. Again, the original CCSM-driven simulations produced a reversed JFM precipitation trend during 1979-1999 in comparison to the PRISM observations, while precipitation trends of both the NCEP-driven and bias-corrected CCSM-driven simulations show the same tendency as PRISM.

We further analyzed 2-meter air temperatures derived from PRISM and WRF simulations (see Figure 5). Evident from the original CCSM-driven simulations is a steep cooling trend; this is evident in all four regions and likely the cause of the marked increase in the original CCSM-driven simulation's SWE trend (Figure 3). Such a cooling trend is contrary to all anthropogenic warming scenarios (including the A2 scenario) but more importantly, is inconsistent with the SNOTEL observations. In the bias-corrected CCSM-driven simulation, the cooling trends were much reduced, though not reversed to the degree of perfect agreement with the observation. The combined improvements (or corrections) in both precipitation and temperature in the bias-corrected CCSM-driven simulations did lead to improvements in the representation of SWE and its trends.

4. Discussion and conclusion

We analyzed the results from three RCM simulations of winter precipitation and snowpack projections to examine the reduction of biases existing in both CGCMs and RCM parameterizations. The biases associated with RCM parameterizations were reduced by selecting an optimal combination of physics schemes through sensitivity tests; and the biases from CGCMs were corrected using a statistical method. It was found that the bias-corrected CCSM data resulted in a more reasonable simulation of the atmospheric circulations. The better representation of the atmospheric circulation dynamics did produce a more realistic precipitation climatology, and this in turn projected a precipitation change that was more closely aligned with the newer generation of multi-model downscaled projections of the CMIP5 (see Brekke et al. 2012, 2013). The precipitation and temperature trends during the historical period were also improved by the bias correction method. Such improvement led to a better simulation of SWE; this is particularly important in the western U.S. where snowmelt accounts for as much as 75% of water supplies (USGS 2014). In addition, the improvement of SWE simulations presented here signifies an economical alternative to reduce the expense of having to perform high-resolution simulations (i.e. < 10 km).

Previous studies, using different combinations of CGCMs and RCMs, have produced different (even opposite) downscaled climate projections for the western U.S. (Dominguez et al. 2012; McAfee et al. 2011;Pierce et al. 2013a; Pierce et al. 2013b; Qian et al. 2010). Such a broad range of climate projections has led to the preference of an ensemble approach in the provision of more agreeable and supposedly more confident climate projections for their applications. However, performing large-ensemble simulations using RCMs is cost-prohibitive. The present study demonstrated that, by employing one RCM forced with bias-corrected lateral boundary conditions obtained from one CGCM, the resulting precipitation and snow downscaling can be as consistent as the multi-model downscaled projections such as those from the CMIP5 (Brekke et al. 2013). Although this study used the CCSM output and the WRF model, the same method can be applied to any other combination of global and regional climate models.

Acknowledgements

We would like to acknowledge our funding from Bureau of Reclamation (project No: R11AC81456 and R13AC80039) in support of this research.

REFERENCES

Brekke, L., D. Raff, K. Werner, K. White, and A. Wood, 2012: Anticipating, Preparing for, and Managing Through Extreme Weather and Climate Events: Water Resource Managers' Needs for Improved Weather and Climate Prediction Information. *10th Annual Climate Prediction Applications Science Workshop,March 13–15, 2012, Miami, Florida, USA,*

Brekke, L., B. Thrasher, T. Pruitt, E. P. Maurer, C. Tebaldi, J. R. Arnold, and J. Long, 2013: New CMIP5 Downscaled Climate and Hydrology Projections. *11th Annual Climate Prediction Applications Science Workshop, April 23-25, 2013, Logan, Utah, USA,*

Christensen, N., A. Wood, N. Voisin, D. Lettenmaier, and R. Palmer, 2004: The effects of climate change on the hydrology and water resources of the Colorado River basin. *Clim. Change,* **62**, 337-363.

Daly, C., R. P. Neilson, and D. L. Phillips, 1994: A Statistical Topographic Model for Mapping Climatological Precipitation Over Mountainous Terrain. *J. Appl. Meteorol.,* **33**, 140-158.

Dettinger, M., D. Cayan, M. Meyer, and A. Jeton, 2004: Simulated hydrologic responses to climate variations and change in the Merced, Carson, and American River basins, Sierra Nevada, California, 1900-2099. *Clim. Change,* **62**, 283-317.

Dominguez, F., E. Rivera, D. P. Lettenmaier, and C. L. Castro, 2012: Changes in winter precipitation extremes for the western United States under a warmer climate as simulated by regional climate models. *Geophys. Res. Lett.,* **39**, L05803.

Gillies, R. R., S. Wang, and M. R. Booth, 2012: Observational and Synoptic Analyses of the Winter Precipitation Regime Change over Utah. *J. Clim.,* **25**, 4679-4698.

Gutierrez, J. M., D. San-Martin, S. Brands, R. Manzanas, and S. Herrera, 2013: Reassessing Statistical Downscaling Techniques for Their Robust Application under Climate Change Conditions. *J. Clim.,* **26**, 171-188.

Hayhoe, K. and Coauthors, 2004: Emissions pathways, climate change, and impacts on California. *Proc. Natl. Acad. Sci. U. S. A.,* **101**, 12422-12427.

Hewitson, B. C., and R. G. Crane, 1996: Climate downscaling: Techniques and application. *Climate Research,* **7**, 85-95.

Holton, JR (1992) An introduction to dynamic meteorology, Third Edition, Academic Press, San Diego, pp. 511.

Howat, I., and S. Tulaczyk, 2005: Climate sensitivity of spring snowpack in the Sierra Nevada. *J. Geophys. Res. -Earth Surf.,* **110**, F04021.

Jin, J., S. Y. Wang, and R. R. Gillies, 2011: Improved Dynamical Downscaling of Climate Projections for the Western United States. *Climate Change: Research and Technology for Adaptation and Mitigation,* J. Blanco and H. Kheradmand eds., InTech, 23-38.

Jin, J., and L. Wen, 2012: Evaluation of snowmelt simulation in the Weather Research and Forecasting model. *Journal of Geophysical Research-Atmospheres,* **117**, D10110.

Kalnay, E. and Coauthors, 1996: The NCEP/NCAR 40-year reanalysis project. *Bull. Am. Meteorol. Soc.,* **77**, 437-471.

Leung, L. R., Y. Qian, and X. D. Bian, 2003: Hydroclimate of the western United States based on observations and regional climate simulation of 1981-2000. part I: Seasonal statistics. *J. Clim.,* **16**, 1892-1911.

Leung, L. R., Y. Qian, X. D. Bian, and A. Hunt, 2003: Hydroclimate of the western

United States based on observations and regional climate simulation of 1981-2000. part II: Mesoscale ENSO anomalies. *J. Clim.,* **16**, 1912-1928.

Liang, X., K. E. Kunkel, G. A. Meehl, R. G. Jones, and J. X. L. Wang, 2008: Regional climate models downscaling analysis of general circulation models present climate biases propagation into future change projections. *Geophys. Res. Lett.,* **35**, L08709.

McAfee, S. A., J. L. Russell, and P. J. Goodman, 2011: Evaluating IPCC AR4 cool-season precipitation simulations and projections for impacts assessment over North America. *Clim. Dyn.,* **37**, 2271-2287.

Mearns, L. O. and Coauthors, 2013: Reply to "Comments on 'THE NORTH AMERICAN REGIONAL CLIMATE CHANGE ASSESSMENT PROGRAM Overview of Phase I Results'". *Bull. Am. Meteorol. Soc.,* **94**, 1077-1079.

Mearns, L. O. and Coauthors, 2012: THE NORTH AMERICAN REGIONAL CLIMATE CHANGE ASSESSMENT PROGRAM Overview of Phase I Results. *Bull. Am. Meteorol. Soc.,* **93**, 1337-1362.

Miller, N. L., K. Hayhoe, J. Jin, and M. Auffhammer, 2008: Climate, extreme heat, and electricity demand in California. *J. Appl. Meteorol. Climatol.,* **47**, 1834-1844.

Nakicenvoic et al., 2000: Special Report on Emissions Scenarios. A Special Report of Working Group III of the Intergovernmental Panel on Climate Change. Cambridge University Press: Cambridge. 599 pp.

Pielke, R. S., 2013: Comments on "THE NORTH AMERICAN REGIONAL CLIMATE CHANGE ASSESSMENT PROGRAM Overview of Phase I Results". *Bull. Am. Meteorol. Soc.,* **94**, 1075-1077.

Pielke, R. A., Sr., and R. L. Wilby, 2012: Regional climate downscaling: What's the point? Eos. Trans. AGU, 93(5), 52.

Pierce, D. W. and Coauthors, 2013a: The Key Role of Heavy Precipitation Events in Climate Model Disagreements of Future Annual Precipitation Changes in California. *J. Clim.,* **26**, 5879-5896.

Pierce, D. W. and Coauthors, 2013b: Probabilistic estimates of future changes in California temperature and precipitation using statistical and dynamical downscaling. *Clim. Dyn.,* **40**, 839-856.

Qian, Y., S. J. Ghan, and L. R. Leung, 2010: Downscaling hydroclimatic changes over the Western US based on CAM subgrid scheme and WRF regional climate simulations. *Int. J. Climatol.,* **30**, 675-693.

Rasmussen, R. and Coauthors, 2011: High-Resolution Coupled Climate Runoff Simulations of Seasonal Snowfall over Colorado: A Process Study of Current and Warmer Climate. *J. Clim.,* **24**, 3015-3048.

Salzmann, N., and L. O. Mearns, 2012: Assessing the Performance of Multiple Regional Climate Model Simulations for Seasonal Mountain Snow in the Upper Colorado River Basin. *J. Hydrometeorol.,* **13**, 539-556.

Subin, Z. M., W. J. Riley, J. Jin, D. S. Christianson, M. S. Torn, and L. M. Kueppers, 2011: Ecosystem Feedbacks to Climate Change in California: Development, Testing, and Analysis Using a Coupled Regional Atmosphere and Land Surface Model (WRF3-CLM3.5). *Earth Interact.,* **15**, 15.

Taylor, K. E., R. J. Stouffer, and G. A. Meehl, 2012: An Overview of CMIP5 and the Experiment Design. *Bull. Am. Meteorol. Soc.,* **93**, 485-498.

USGS, 2014: Snowmelt - The Water Cycle (available at http://water.usgs.gov/edu/watercyclesnowmelt.html). accessed on June 10, 2014.

Wang, S., R. R. Gillies, E. S. Takle, and W. J. Gutowski Jr., 2009: Evaluation of precipitation in the Intermountain Region as simulated by the NARCCAP regional climate models. *Geophys. Res. Lett.,* **36**, L11704.

Wilby, R. L., T. M. L. Wigley, D. Conway, P. D. Jones, B. C. Hewitson, J. Main, and D. S. Wilks, 1998: Statistical downscaling of general circulation model output: A comparison of methods. *Water Resour. Res.,* **34**, 2995-3008.

Wood, A. W., L. R. Leung, V. Sridhar, and D. P. Lettenmaier, 2004: Hydrologic implications of dynamical and statistical approaches to downscaling climate model outputs. *Clim. Change,* **62**, 189-216.

List of Tables

List of Figures

Figure 1: Mean JFM precipitation in 1969-1999 from (a) the PRISM data, (b) NCEP-driven, (c) original CCSM-driven, and (d) corrected CCSM-driven WRF simulations, as well as the JFM precipitation differences between the years 2056-2065 and 2001-2010 for the (e) original and (f) bias-corrected CCSM-driven simulations. Units: mm month-1. The boxes labeled 1, 2, 3, and 4 in Figure 1b delineate four mountain regions: (1) the Cascade Range, (2) the Bitterroot Range, (3) the Wasatch Range, and (4) the Colorado Rockies.

Figure 2: Mean JFM wind fields at 200 hPa in 1969-1999 simulated using (a) the NCEP as well as (b) original and (c) bias-corrected CCSM data. The differences in JFM wind fields at 200 hPa between the years 2056-2065 and 2001-2010 for the (d) original and (e) bias-corrected CCSM-driven simulations. The differences in JFM wind fields at 600 hPa between the years 2056-2065 and 2001-2010 for the (f) original and (g) bias-corrected CCSM-driven simulations. Units: m s^{-1}.

Figure 3: The time series (for all years — i.e. 1969-1999, 2001-2010, and 2056-2065) of region-wide average April 1 SWE for Regions 1 through 4. The black line represents observed April 1 SWE averaged over all SNOTEL stations in each region. The green, blue, and red lines represent the region-wide average April 1 SWE simulated by WRF driven by the NCEP, the original and bias-corrected CCSM (lateral boundary conditions), respectively.

Figure 4: The time series (for all years — i.e. 1969-1999, 2001-2010, and 2056-2065) of region-wide average JFM precipitation for Regions 1 through 4. The black line represents observed JFM precipitation from PRISM in each region. The green, blue, and red lines represent the region-wide average JFM precipitation simulated by WRF using the NCEP, the original and bias-corrected CCSM, respectively.

Figure 5: The time series (for all years — i.e. 1969-1999, 2001-2010, and 2056-2065) of region-wide average JFM surface temperature for Regions 1 through 4. The black line represents observed JFM surface temperature from PRISM in each region. The green, blue, and red lines represent the region-wide average JFM surface temperature simulated by WRF using the NCEP, the original and bias-corrected CCSM, respectively.

Table 1. The optimal set of physics schemes adopted in this study: long-wave (LW) and short-wave (SW) radiation (RA), land surface (LS), microphysics (MP), cumulus (CU), and planetary boundary layer (PBL) schemes

		Scheme	Major characteristics
RA	LW	Rapid Radiative Transfer Model (RRTM)	K-distribution method with 256 g points
	SW	Dudhia	Calculation of clear-air scattering, water vapour absorption, and cloud albedo and absorption using look-up tables for clouds
LS		Community Land Model (CLM)	Sophisticated ten-layer temperature and moisture soil model with detailed vegetation representation
MP		Goddard	Simulates water vapour and condensate, into which the following four hydrometeor fields are combined for advection calculations: cloud water, rain, cloud ice, and precipitation ice
CU		Grell-Devenyi ensemble	One-dimensional mass flux scheme that consists of a single updraft–downdraft couplet
PBL		Bougeault and Lacarrere (BouLac)	TKE closure scheme in which vertical diffusion coefficient for momentum, the coefficient for heat, and the coefficient for TKE are identical

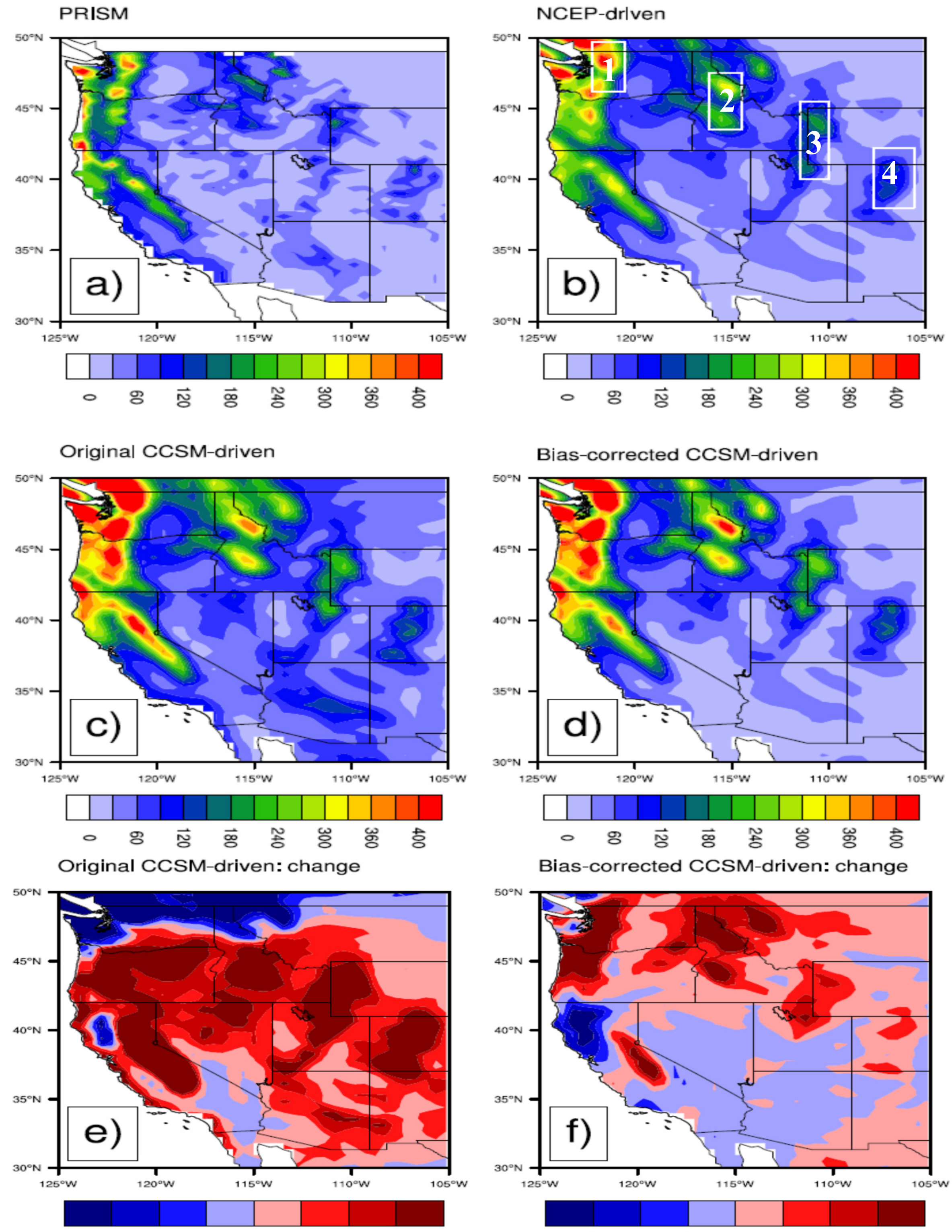

Figure 1: Mean JFM precipitation in 1969-1999 from (a) the PRISM data, (b) NCEP-driven, (c) original CCSM-driven, and (d) corrected CCSM-driven WRF simulations, as well as the JFM precipitation differences between the years 2056-2065 and 2001-2010 for the (e) original and (f) bias-corrected CCSM-driven simulations. Units: mm month^{-1}. The boxes labeled 1, 2, 3, and 4 in Figure 1b delineate four mountain regions: (1) the Cascade Range, (2) the Bitterroot Range, (3) the Wasatch Range, and (4) the Colorado Rockies.

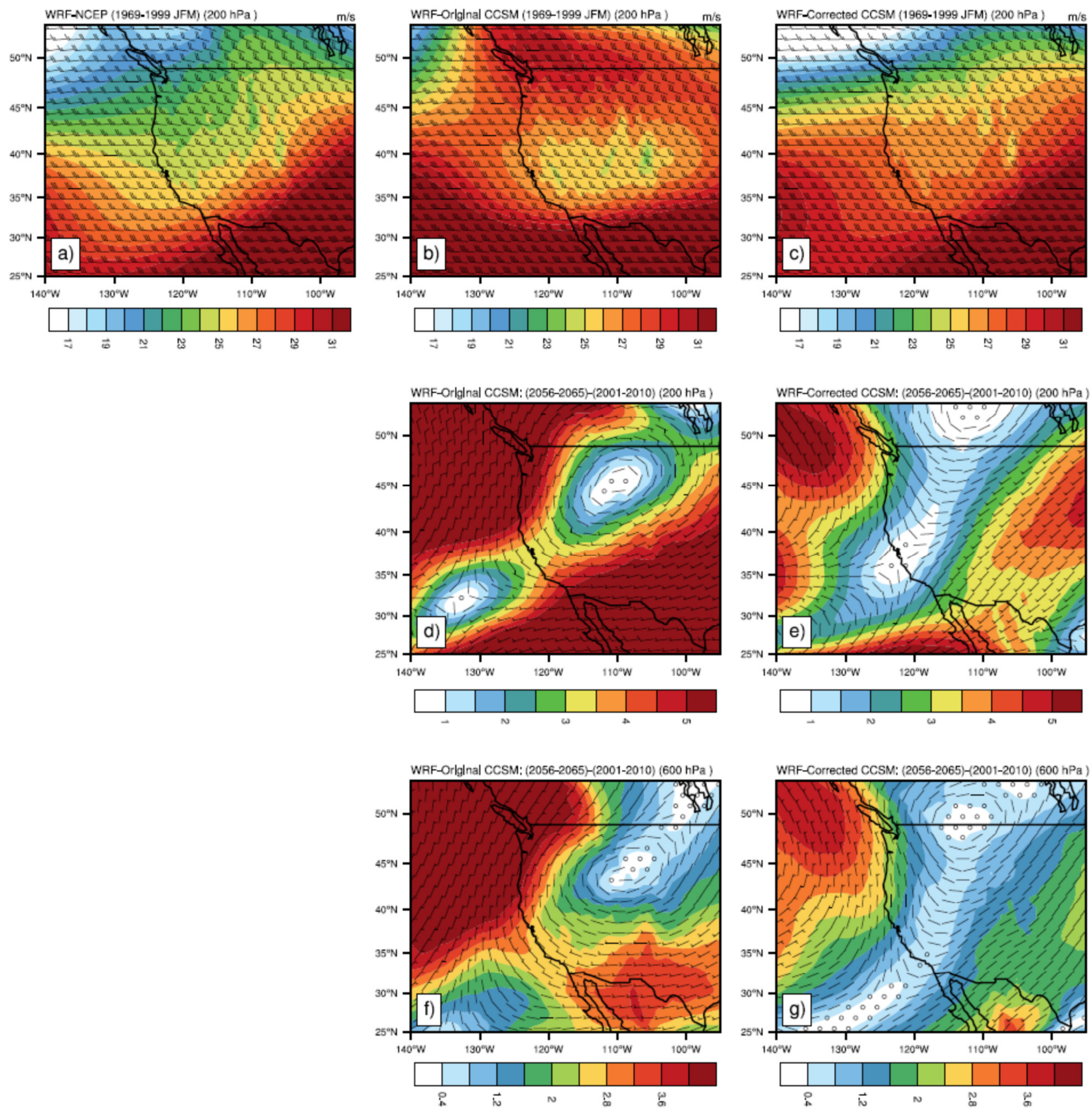

Figure 2: Mean JFM wind fields at 200 hPa in 1969-1999 simulated using (a) the NCEP as well as (b) original and (c) bias-corrected CCSM data. The differences in JFM wind fields at 200 hPa between the years 2056-2065 and 2001-2010 for the (d) original and (e) bias-corrected CCSM-driven simulations. The differences in JFM wind fields at 600 hPa between the years 2056-2065 and 2001-2010 for the (f) original and (g) bias-corrected CCSM-driven simulations. Units: m s^{-1}.

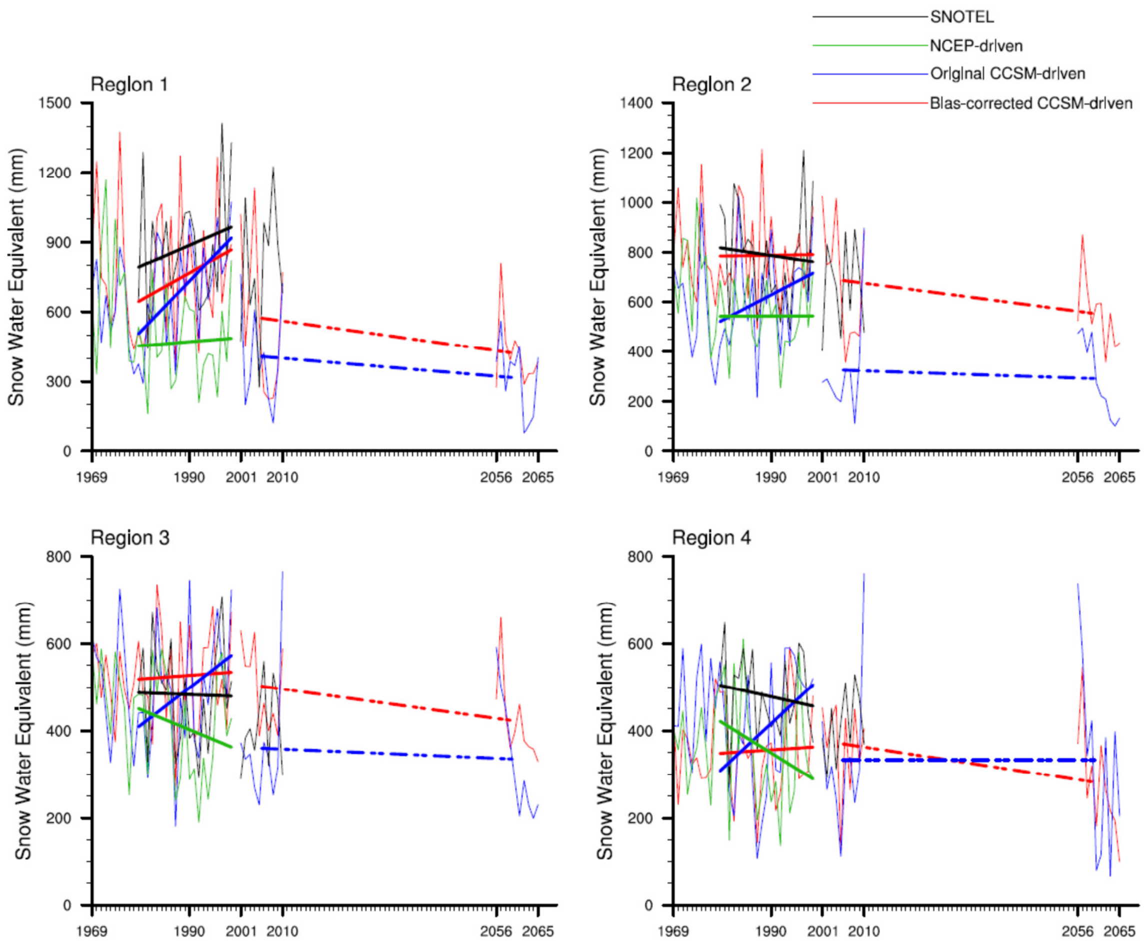

Figure 3: The time series (for all years — i.e. 1969-1999, 2001-2010, and 2056-2065) of region-wide average April 1 SWE for Regions 1 through 4. The black line represents observed April 1 SWE averaged over all SNOTEL stations in each region. The green, blue, and red lines represent the region-wide average April 1 SWE simulated by WRF driven by the NCEP, the original and bias-corrected CCSM (lateral boundary conditions), respectively.

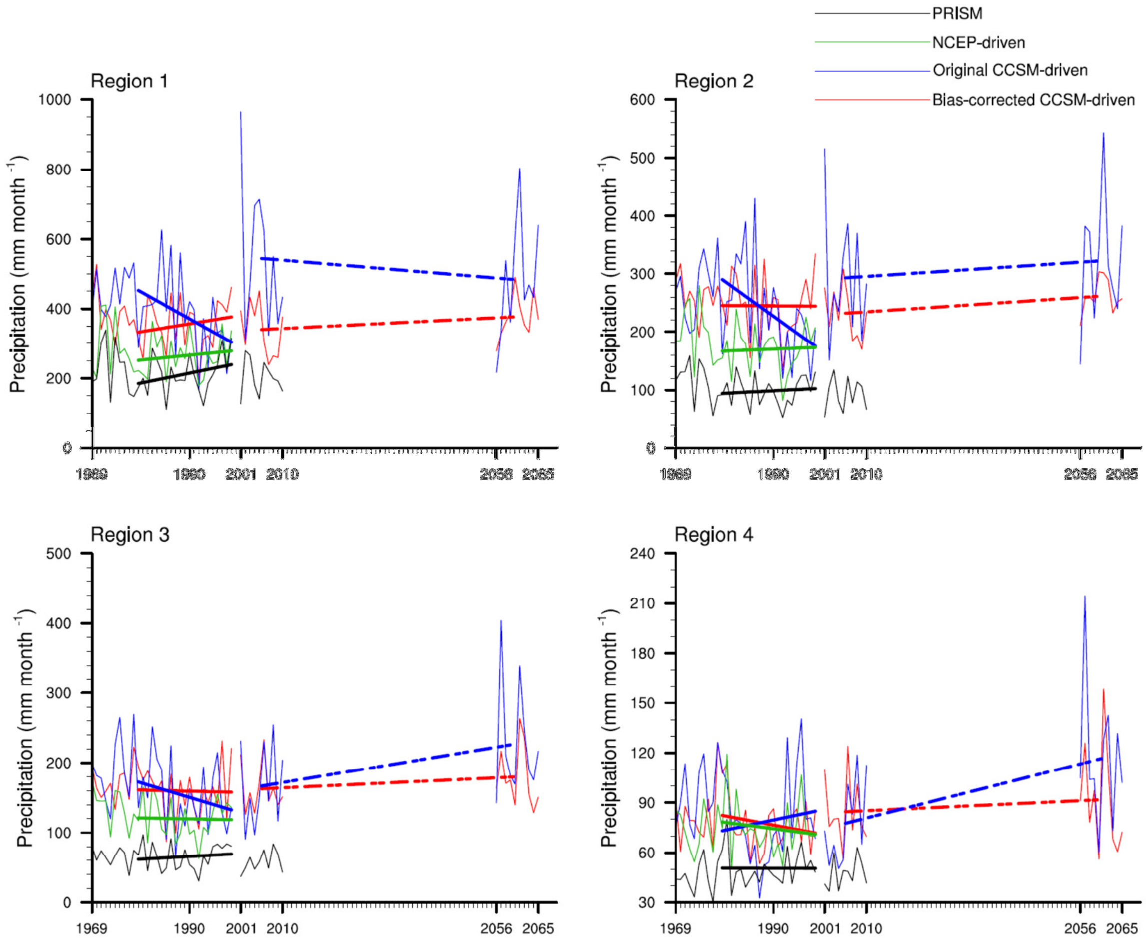

Figure 4: The time series (for all years — i.e. 1969-1999, 2001-2010, and 2056-2065) of region-wide average JFM precipitation for Regions 1 through 4. The black line represents observed JFM precipitation from PRISM in each region. The green, blue, and red lines represent the region-wide average JFM precipitation simulated by WRF using the NCEP, the original and bias-corrected CCSM, respectively.

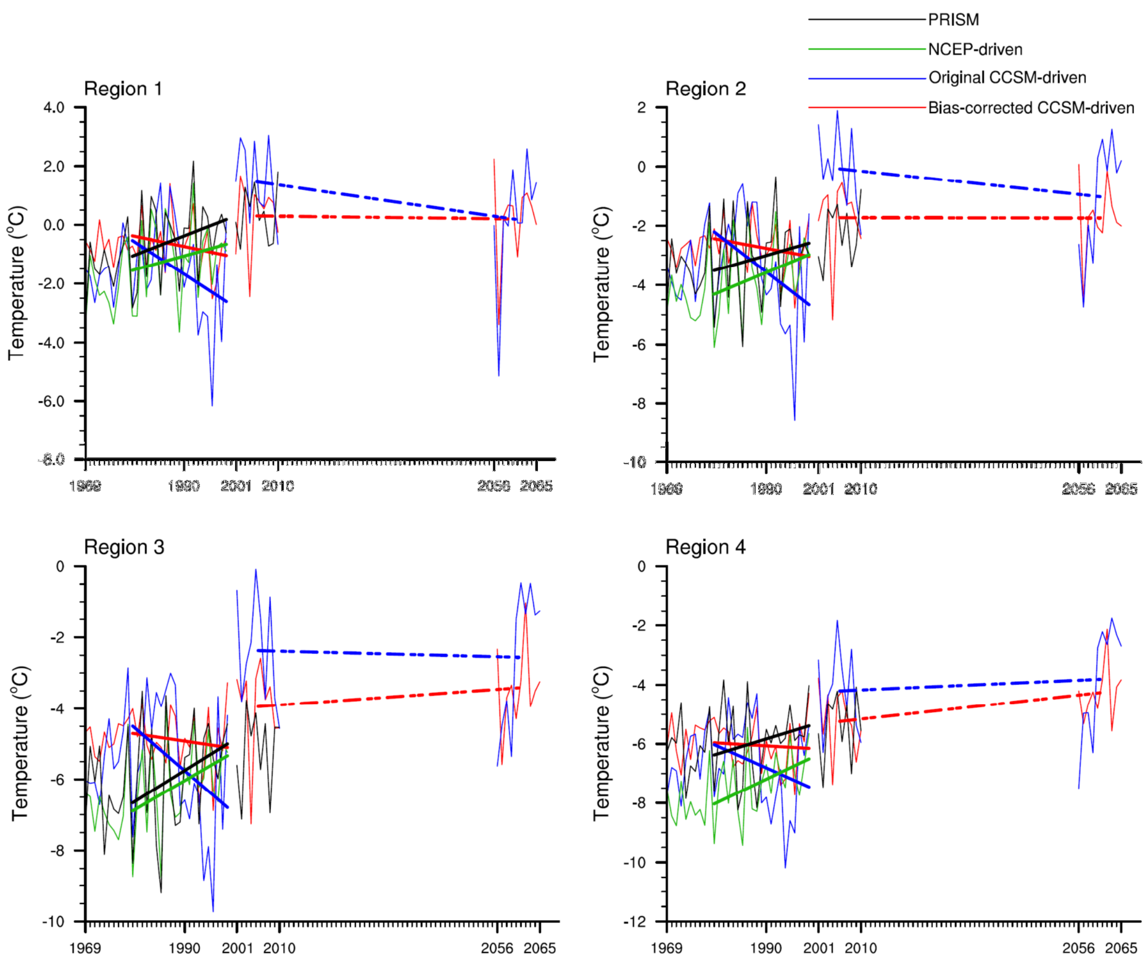

Figure 5: The time series (for all years — i.e. 1969-1999, 2001-2010, and 2056-2065) of region-wide average JFM surface temperature for Regions 1 through 4. The black line represents observed JFM surface temperature from PRISM in each region. The green, blue, and red lines represent the region-wide average JFM surface temperature simulated by WRF using the NCEP, the original and bias-corrected CCSM, respectively.